Current Biology *18*, 1338–1343, September 9, 2008 DOI 10.1016/j.cub.2008.07.075

Report

The Balance between CONSTANS and TEMPRANILLO Activities Determines *FT* Expression to Trigger Flowering

Cristina Castillejo[1] and Soraya Pelaz[1,2,*]
[1]Centre for Research in Agricultural Genomics
CSIC-IRTA-UAB
Jordi Girona 18
08034 Barcelona
Spain
[2]ICREA (Institució Catalana de Recerca i Estudis Avançats)
08010 Barcelona
Spain

Summary

Seasonal changes in day length influence flowering time in many plant species. In *Arabidopsis*, flowering is accelerated by exposure to long day (LD). Those inductive photoperiods are perceived in leaves [1] and initiate a long-distance signaling mediated by CO and FT. *CO* is expressed in the phloem according to a circadian rhythm [2–4]. Only under LD does CO induce *FT* expression as high levels of *CO* in the evening coincide with the external light that stabilizes CO protein [4, 5]. Subsequently, FT protein travels through the phloem to the shoot apex where, together with FD, it initiates flowering [6–12]. Despite the photoperiodic induction, a mechanism of floral repression is needed to avoid precocious flowering. We show that *TEMPRANILLO* genes (*TEM1* and *TEM2*) act as novel direct *FT* repressors. Molecular and genetic analyses suggest that a quantitative balance between the activator CO and the repressor TEM determines *FT* levels. Moreover, developmental *TEM* downregulation marks the timing of flowering, as it shifts the CO/TEM balance in favor of CO activity, allowing *FT* transcript to reach the threshold level required to trigger flowering. We envision that this might be a general mechanism between long-day plants to ensure a tight regulation of flowering time.

Results and Discussion

TEM1 (*At1g25560*) and *TEM2* (*At1g68840; RAV2*) belong to the *RAV* (related to ABI3/VP1) subfamily of transcription factors, which comprises six genes in *Arabidopsis* [13] (Figure S1 available online). RAV proteins contain two DNA-binding domains, an AP2/ERF and a B3 DNA-binding domain, although currently neither their target genes nor the action mechanisms are known.

TEM function was investigated with a genetic approach. Loss of function was analyzed in the RNA null allele *tem1-1* that has a T-DNA insertion 3 bp after the initiation codon (Figure S2A). The *tem1-1* mutation promoted a subtle early flowering phenotype in LD, which raised the possibility of a functional redundancy. *TEM2* is the closest homolog of *TEM1* (Figure S1); however, no null allele of *TEM2* was available. To overcome this problem, *Arabidopsis* plants were transformed with an RNA interference (RNAi) construct that targeted both genes. Of 10 independent lines analyzed, we selected two of them that differed in the degree of silencing of *TEM1* and *TEM2* (Figure S2A). *TEM* expression levels correlated with the flowering phenotype as shown by the fact that the RNAi-*tem2* lines did not show any phenotype and only the double RNAi-*tem1/2* flowered earlier than the single *tem1-1* mutant (Figure 1B). Apart from the precocious flowering, the RNAi-*tem1/2* plants showed a slight reduction in leaf size that was not seen in RNAi *tem2* or *tem1*-1 plants (Figure 1A). The phenotype of these RNAi-*tem1/2* plants was not due to an additional reduction of other close *RAV* genes because the closest *RAV1* gene is normally expressed (Figure S2B). Also an Agrikola [13] RNAi-*tem2* line that had a great reduction in *TEM2* levels (Figure S2A) did not show any phenotype but when combined with *tem1*-1 enhanced the *tem1* early flowering phenotype (not shown).

We then generated transgenic plants overexpressing *TEM* genes. Both 35S::*TEM1* and 35S::*TEM2* (Figure 1C) plants showed the same phenotype and flowered extremely late under LD conditions. Most of the 35S::*TEM* plants bolted 5 weeks later than in the wild-type and produced at least 10 extra rosette leaves before flowering, although the exact number of leaves could not be estimated because of the large number of axillary leaves and secondary rosettes. A dose effect was also observed in the 35S::*TEM* plants as the homozygotes displayed a stronger phenotype than the hemizygotes (not shown).

For simplicity, we concentrated our studies on *TEM1* function. The first evidence of TEM1 acting as a putative *FT* regulator came from the double 35S::*TEM1 lfy-26* plants, which showed an identical phenotype to double *ft lfy* mutants [11, 12, 14] (Figures S3A and S3B). We then found that indeed *FT* levels greatly decreased in 35S::*TEM1* plants and increased in *tem1-1* and RNAi-*tem1/2* plants (Figure S3C; Figures 1D and 1E). Those changes in *FT* abundance were not due to a phase shift in the *FT* diurnal cycling (Figure 1D), and therefore we concluded that TEM1 was repressing *FT.* Consequences of altered *TEM1* expression on *FT* levels were analyzed during development. In wild-type seedlings, *FT* mRNA remained at basal levels until day 8 but around the transition to flowering, at days 10–12, there was a pronounced increase in *FT* accumulation. This peak of *FT* expression, responsible for floral induction, was abolished in the 35S::*TEM1* seedlings so the switch to flowering did not occur. By contrast, in *tem1-1*, *FT* levels increased earlier than in the wild-type. 8-day-old *tem1-1* plants had already reached the *FT* levels of a 10-day-old wild-type plant, and consequently flowering was accelerated (Figure 1E). Consistent with *FT* acting downstream of *TEM1*, the late flowering phenotype of 35S::*TEM1* plants was completely suppressed by the constitutive expression of *FT* (Figure 1F). The combination of loss-of-function alleles of *TEM1* and *FT* further confirmed the epistatic relationship between both genes as the double mutant *tem1-1 ft-101* flowered at the same time as *ft-101* alone (Figure 1F). These results also suggest that *FT* is the primary downstream target of TEM1 to repress flowering.

To further understand the relationship between *TEM1* and *FT*, we compared their expression patterns with pTEM1::*GUS* and pFT::*GUS* plants. pTEM1*::GUS* was detected in all vegetative tissues. In leaves, *TEM1* is expressed both in vascular and

*Correspondence: soraya.pelaz@ibmb.csic.es

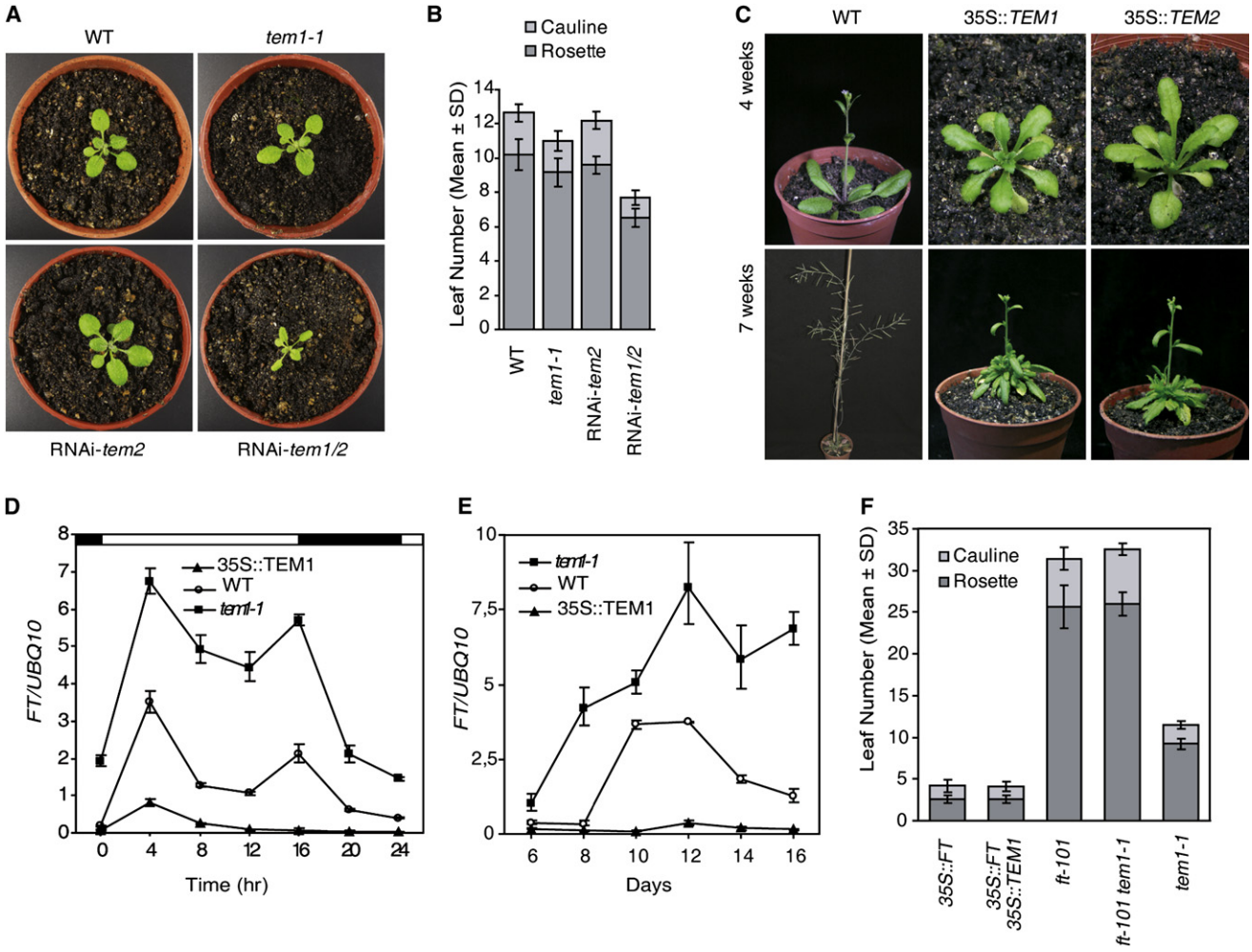

Figure 1. *TEM* Genes Delay Flowering and Repress *FT* Expression

(A) Vegetative phenotype of 15-day-old *tem1-1* and RNAi-*tem* plants.

(B) Flowering time of *tem1-1* under LD. Error bars are the standard deviation (SD) of the mean number of leaves (rosette and cauline).

(C) Flowering phenotype of 35S::*TEM* plants. The earliest plants started bolting 3 weeks later than the WT.

(D) *FT* circadian expression in WT, *tem1-1*, and 35S::*TEM1* plants under LD. qRT-PCR was performed in samples collected during day 9.

(E) qRT-PCR of *FT* through development in WT, *tem1-1*, and 35S::*TEM1*. Error bars in (D) and (E) are the SD of the mean of three qRT-PCR replicates.

(F) *FT* is epistatic to *TEM1*. 35S::*FT* totally suppressed the 35S::*TEM1* late flowering phenotype and *ft-101* suppressed the early flowering phenotype of *tem1-1*. Error bars are the standard deviation (SD) of the mean number of leaves (rosette and cauline).

mesophyll tissues although the levels and spatial distribution changed through development (Figure 2A). We focused on the dynamics of the expression in the first true leaf, representative of what occurs in the rest of the leaves. In agreement with the role of TEM1 as an *FT* repressor, both genes followed a temporarily antagonistic expression pattern although some spatial overlap occurs. In 6-day-old plants, *TEM1* expression was very high in the whole leaf whereas *FT* was hardly detected. Later on, *TEM1* started clearing from the leaf, at the same time as *FT* increased its expression, and continued declining until *FT* reached its maximum at day 12, around floral transition (Figure 2A).

A qRT-PCR time-course analysis of *TEM1* was performed to better quantify those changes in *TEM1* levels throughout development (Figure 2B). Consistent with the pTEM1*::GUS* results, *TEM1* mRNA abundance was very high during early stages of seedling development but a pronounced decline took place just before floral transition. *CO* and *FT* expression were also monitored over this same time period. We observed that *CO* expression remained almost unaltered through development, although a subtle increase occurred during the transition to flowering. Thus, changes in *CO* and *TEM1* expression were reflected in *FT* levels, which reached the threshold level necessary to trigger flowering around days 10–12, coinciding with the slight upregulation of *CO* and once *TEM1* levels had dropped (Figure 2B). *TEM1* downregulation is independent of FT as shown by the fact that *TEM1* expression was almost unaffected in *ft*-101 or 35S::*FT* plants (Figure S4).

We also tested whether *TEM1* expression follows a diurnal oscillation like *CO*. Under LDs, *TEM1* abundance was low during the daytime and peaked at dusk (Figure 2C). This daily cycling of *TEM1* was controlled by the circadian clock as *TEM1* expression in plants entrained under a 12 hr photoperiod (12 hr light/12 hr dark) for 7 days and then transferred to constant light (LL) continued cycling with an approximately 24 hr period for the next 72 hr (Figure 2D). In addition, the same

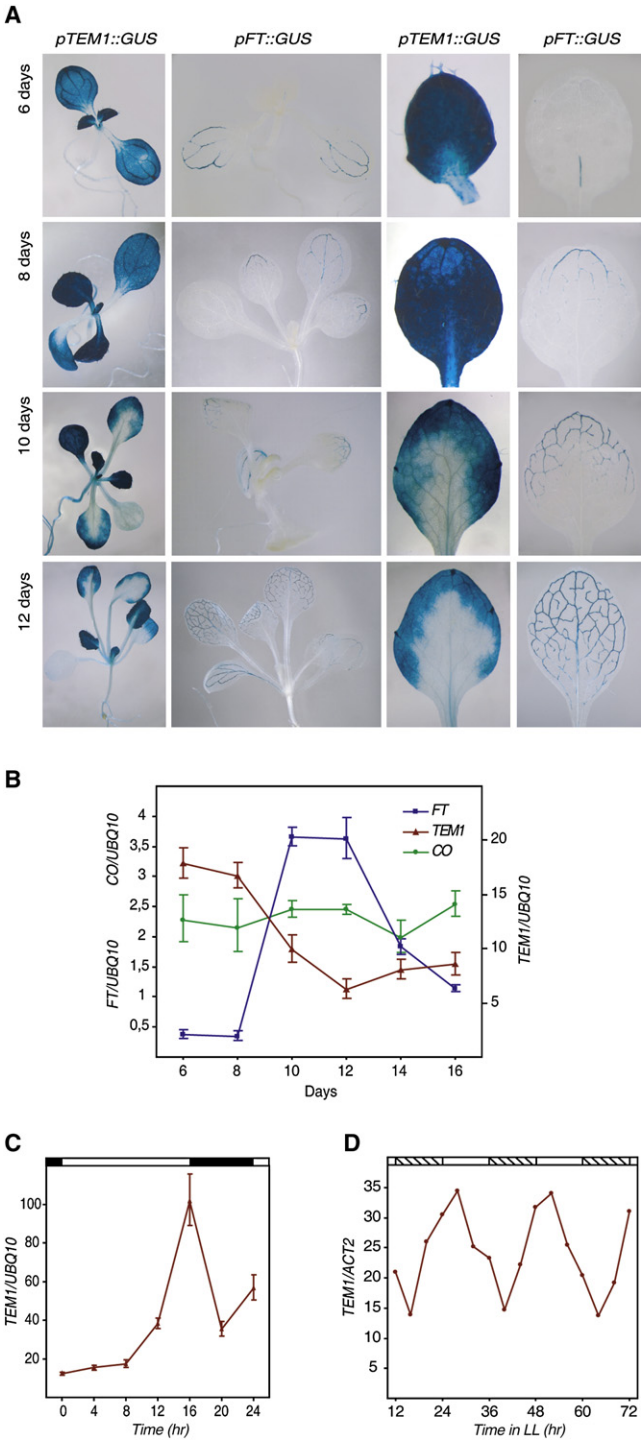

Figure 2. Expression Pattern of *TEM1*

(A) GUS accumulation in *pTEM1::GUS* and *pFT::GUS* plants under LD. Columns furthest right show a magnification of the first true leaf.
(B) qRT-PCR time course analysis of *TEM1*, *CO*, and *FT* expression in LD.
(C) Diurnal cycling of *TEM1* under LD. Samples were collected during day 8. Error bars in (B) and (C) are the SD of the mean of three qRT-PCR replicates.
(D) Northern analysis of *TEM1* expression under LL.

developmental and circadian regulation of *TEM1* was observed for *TEM2*, supporting the proposed redundant role of both genes (Figure S5).

Despite the current knowledge about the mechanism of photoperiodic induction of flowering, a question that remains unclear is why *Arabidopsis* plants take a couple of weeks to flower in LD. In those conditions, CO is expressed and active since the very beginning of the development, and changes in *CO* expression levels do not seem enough to account for the increase in *FT* accumulation (Figure 2B). Alternatively, the *TEM* expression pattern suggested that the balance between TEM and CO activities might be modulating *FT* levels and consequently adjusting the timing of floral transition under inductive photoperiods. Besides, as both *CO* and *TEM* are regulated by the circadian clock, they could be acting on *FT* at the same level but antagonistically. The importance of the proposed CO/TEM balance was manifested under circumstances in which this balance was impaired (Figure 3). In LD-grown plants, an increase in the amount of CO had the same effect on flowering as did the removal of the repressor, as suggested by the almost identical precocious flowering phenotype of 35S::*CO* and RNAi-*tem1/2* plants. LD-grown 35S::*CO* plants flowered after producing a total of 7.0 ± 1.1 leaves compared to 7.7 ± 0.9 leaves of the RNAi-*tem1/2* plants. A higher reduction in the repressor amount, that is, RNAi-*tem1/2 tem1*-1 plants, did not further reduce the flowering time, so perhaps it is not possible to flower earlier unless *FT* is directly activated as in 35S::*FT* plants. However, when both *CO* and *TEM* levels were elevated, in 35S::*CO* 35S::*TEM1* plants, the balance between the activator and the repressor was restored and consequently these plants flowered after producing a wild-type number of leaves (Figures 3A and 3B). A dose effect was also evident in 35S::TEM1/+ 35S::*CO* plants as shown by the fact that they flowered at an intermediate time between 35S::*CO* and 35S::*CO* 35S::*TEM1* or wild-type plants (Figure 3B). In addition, we scored flowering time of plants with reduced CO and TEM activities. *co* heterozygote plants display a slight haplo-insufficient phenotype and flower later than the wild-type [15] (Figure 3D). This phenotype was suppressed by reducing *TEM* abundance in *co-101*/+ plants and thus *co-101*/+ RNAi-*tem1/2* plants flowered at the same time as the wild-type plants (Figure 3D). Notably, *FT* accumulation in the respective crosses correlated with the flowering phenotypes (Figures 3C and 3E).

The next question to address was whether *FT* was a direct target of TEM1. The CAACA and CACCTG sequences have previously been identified as the DNA recognition sites of RAV1 [16]. The presence of these motifs in the 5′UTR region of *FT* gene suggested that TEM1 could be directly repressing *FT.* This interaction was confirmed by EMSA assays with a GST-TEM1 fusion protein and a *FT* DNA probe that included the predicted binding sites (Figure 4A). Excess wild-type, but not mutant, competitors totally eliminated the retardation band, indicating the high specificity of the interaction and that intact AP2-like and B3-like binding sites are necessary for optimal DNA binding of TEM1 (Figure 4A). The binding of TEM1 to the *FT* 5′UTR was further corroborated in vivo by chromatin immunoprecipitation (ChIP) on our 35S::*TEM1* lines, which express the TEM1:HA fusion protein. DNA was immunoprecipitated with an HA antibody and analyzed by qRT-PCR via two primer sets specific for the *FT* promoter region. As shown in Figure 4C, we succeeded in effectively immunoprecipitating a fragment of *FT* that contains the putative TEM1 binding sites but not another one located 2500 bp upstream of the ATG. Strikingly, the RAV binding site in *FT* is located right beside the CAAT element found 43 bp upstream of the ATG (Figure 4B). This CAAT has been suggested as a putative

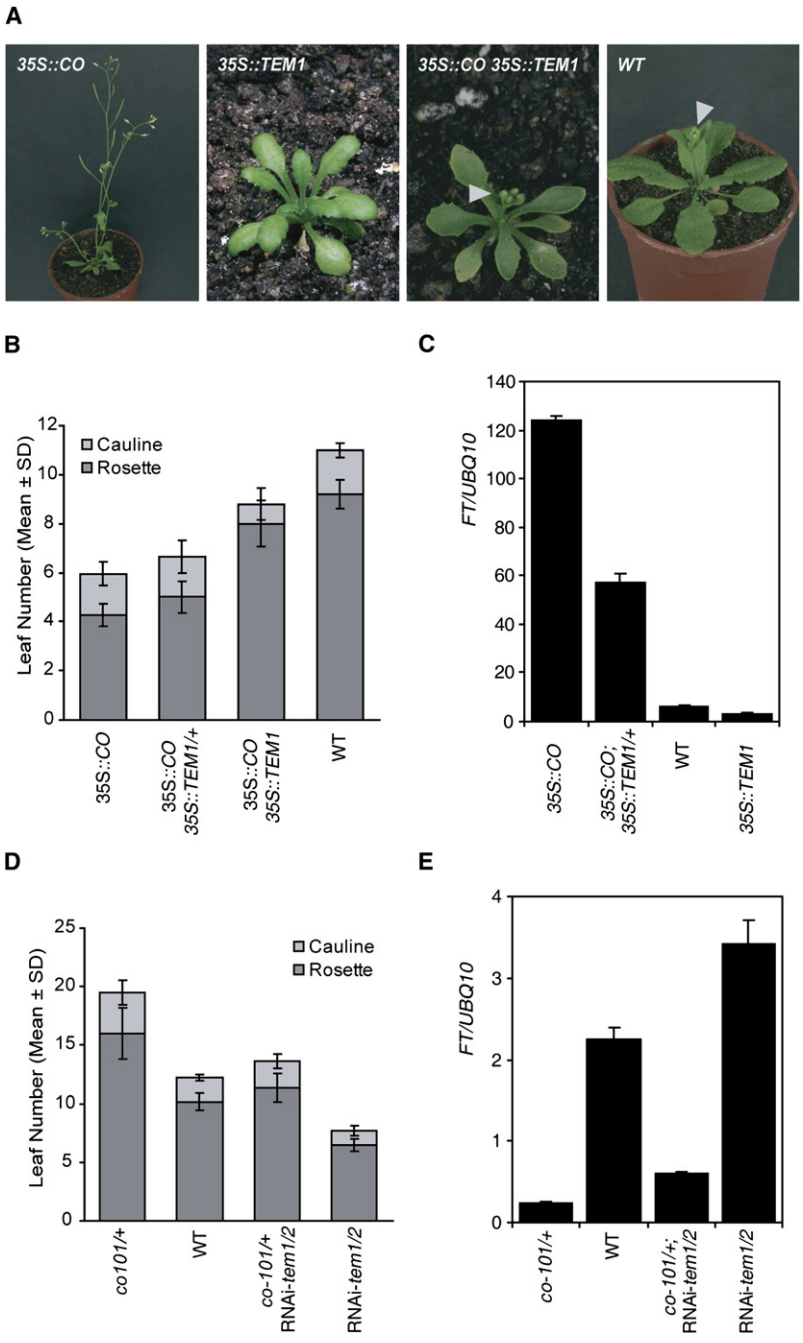

Figure 3. Antagonistic Effect of CO and TEM Activities on Flowering Time and *FT* Expression

(A) Flowering phenotypes of 4-week-old 35S::*CO*, 35S::*TEM1*, 35S::*CO* 35S::*TEM1*, and WT plants. Arrowheads point to the just arisen inflorescences of 35S::*CO* 35S::*TEM1* and WT plants.

(B) Flowering time of 35S::*CO*, 35S::*CO* 35S::*TEM1*/+, 35S::*CO* 35S::*TEM1*, and WT plants.

(C) qRT-PCR of *FT* in WT, 35S::*CO*, 35S::*TEM1*, and 35S::*CO* 35S::*TEM1*/+ 10-day-old plants. *FT* levels correlated with the flowering phenotypes shown in (A) and (B).

(D) Flowering time of *co-101*/+, WT, *co-101*/+ RNAi-*tem1/2*, and RNAi-*tem1/2* plants under LD. Error bars in (B) and (D) are the SD of the mean number of leaves (rosette and cauline).

(E) qRT-PCR of *FT* in the genotypes shown in (D). Seedlings were collected at day 10. Error bars in (C) and (E) are the SD of the mean of three qRT-PCR replicates.

binding site for the complex formed by CO and the CCAAT box binding proteins involved in the activation of *FT* [17]. Therefore, it is tempting to speculate about a possible mechanism that would involve a competition between the CO complex and TEM for the respective binding sites to directly regulate *FT* accumulation and allow a precise control of flowering time.

In conclusion, our studies provide molecular and genetic evidence for an essential function of TEM as a repressor of *FT* expression via direct binding to its 5′UTR region. We propose that the circadian clock output pathway that promotes photoperiod-dependent flowering comprise the antagonistic CO and TEM activities. Hence *FT* levels are the result of a quantitative balance between the respective promoter and repressive activities. Furthermore, we show that downregulation of *TEM* expression is necessary to provide the plant with the competence to respond to inductive photoperiods, as it enables enough *FT* accumulation. *TEM1* is widely expressed in leaves where the photoperiodic induction of flowering is initiated. Preceding floral transition, some spatial overlap was observed between *TEM* and *FT* expression in the outer part of the leaves. *CO* is also expressed in those cells [2, 3]; however, at that time *TEM* levels are low so probably this TEM amount may not be enough to avoid *FT* activation by CO. This is compatible with the proposed model of the CO/TEM balance.

The proposal that flowering is a process controlled by a quantitative balance between flower-inducing and -inhibiting substances arose from classical physiological studies on the photoperiodic response. These works concluded that several transmissible promoters ("florigen") as well as transmissible and non-transmissible inhibitors ("antiflorigen") allow floral induction when the balance is shifted in favor of "florigen" [1]. Currently, the nature of at least one component of the florigen is perfectly established (for a recent review see [18]) but the antiflorigen substance(s) is still poorly understood. The existence of floral transition repressors possesses a great importance for plant development as they guarantee a vegetative phase long enough to allow necessary energy reserves to be accumulated [19] and also ensure a strict control of flowering time. Although we can not exclude a role for TEM proteins in other floral pathways with different target genes, our results suggest a putative role of TEM proteins as at least part of the so-called antiflorigen substance.

Experimental Procedures

Details of the plant material and constructs used in this work are provided in the Supplemental Data.

Growing Conditions

For analysis of flowering time, plants were grown on soil at 22°C under LD (16 hr light/8 hr dark) photoperiod. At least 10 plants per genotype were included in each experiment.

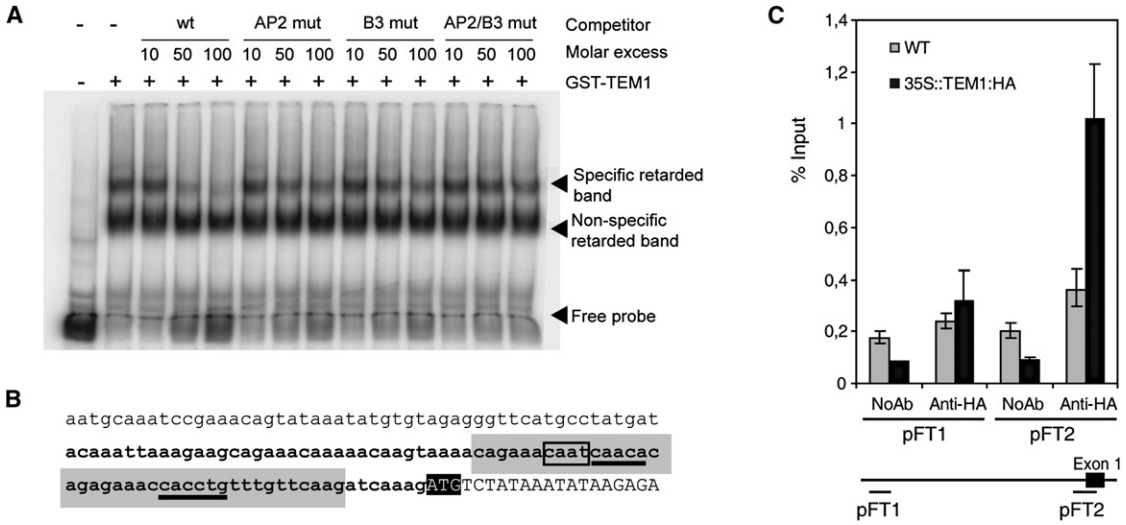

Figure 4. *FT* Is a Direct Target of TEM1

(A) EMSA assay showing the specific binding of TEM1 to the 5′UTR of *FT*.

(B) Sequence and features located upstream the ATG of *FT* gene. 5′ UTR is in bold type. Gray shaded region marks the fragment used for competition in the EMSA assay. Underlined, the CAACA and CACCTG sequences corresponding to the AP2 and B3 binding sites. In a box, the CAAT-box suggested as a putative binding site for the CO/HAP complex.

(C) ChIP analysis of TEM1 binding to *FT* promoter. qRT-PCR was performed on the precipitates by two primer sets. pFT1 amplifies a region 2500 bp upstream the ATG; pFT2 amplifies the region that contains the putative TEM1 binding site. Immunoprecipitated chromatin is enriched in the pFT2 fragment. Error bars correspond to SD of the mean of at least three qRT-PCR replicates.

For time-course expression analysis, plants were grown on Murashige and Skoog (MS) agar medium supplemented with 1% sucrose. Plants were sown at a density of 20 seeds per 8.5 cm plate to ensure a synchronous development. After 2–4 days of seed stratification at 4°C, plates were transferred to the growing chamber at 22°C and LD conditions (16 hr light/8 hr dark). Day 0 was defined as the first day after stratification.

Expression Analyses

All the expression analyses were performed by quantitative real-time PCR (qRT-PCR) except the circadian *TEM1* and *TEM2* expression under LL, which was northern analyzed. Unless indicated, all samples were collected at time 12 after dawn (0 hr).

Detailed information about primers and the protocols followed for qRT-PCR and northern analysis has been included in the Supplemental Data.

The in situ hybridization protocol has been described elsewhere [20].

Binding Assays

EMSA and chromatin immunoprecipitation (ChIP) procedures are detailed in the Supplemental Data.

Supplemental Data

Supplemental Data include Supplemental Experimental Procedures and five figures and are available at http://www.current-biology.com/cgi/content/full/18/17/1338/DC1/.

Acknowledgments

We thank J.M. Casacuberta, C. Loot, M. Perales, and P. Más for technical advice and help; F. Parcy for the donation of pALLI2 vector; K. Goto, G. Coupland, P.A. Wigge, and NASC for seeds; P. Suárez-López for helpful discussions; and T. Jack, P. Suárez-López, D. Weigel, J.M. Casacuberta, and M. Yanofsky for critical reading of the manuscript. This work was supported by a MEC grant (BFU2006-00771) and C.C. by Junta de Andalucía and CRAG.

Received: May 9, 2008
Revised: July 2, 2008
Accepted: July 17, 2008
Published online: August 21, 2008

References

1. Bernier, G. (1988). The control of floral evocation and morphogenesis. Annu. Rev. Plant Physiol. Plant Mol. Biol. *39*, 177–219.
2. An, H., Roussot, C., Suarez-Lopez, P., Corbesier, L., Vincent, C., Pineiro, M., Hepworth, S., Mouradov, A., Justin, S., Turnbull, C., and Coupland, G. (2004). CONSTANS acts in the phloem to regulate a systemic signal that induces photoperiodic flowering of *Arabidopsis*. Development *131*, 3615–3626.
3. Takada, S., and Goto, K. (2003). Terminal flower2, an *Arabidopsis* homolog of heterochromatin protein1, counteracts the activation of flowering locus T by constans in the vascular tissues of leaves to regulate flowering time. Plant Cell *15*, 2856–2865.
4. Suarez-Lopez, P., Wheatley, K., Robson, F., Onouchi, H., Valverde, F., and Coupland, G. (2001). CONSTANS mediates between the circadian clock and the control of flowering in *Arabidopsis*. Nature *410*, 1116–1120.
5. Valverde, F., Mouradov, A., Soppe, W., Ravenscroft, D., Samach, A., and Coupland, G. (2004). Photoreceptor regulation of CONSTANS protein in photoperiodic flowering. Science *303*, 1003–1006.
6. Lin, M.K., Belanger, H., Lee, Y.J., Varkonyi-Gasic, E., Taoka, K., Miura, E., Xoconostle-Cazares, B., Gendler, K., Jorgensen, R.A., Phinney, B., et al. (2007). FLOWERING LOCUS T protein may act as the long-distance florigenic signal in the cucurbits. Plant Cell *19*, 1488–1506.
7. Mathieu, J., Warthmann, N., Kuttner, F., and Schmid, M. (2007). Export of FT protein from phloem companion cells is sufficient for floral induction in *Arabidopsis*. Curr. Biol. *17*, 1055–1060.
8. Jaeger, K.E., and Wigge, P.A. (2007). FT protein acts as a long-range signal in *Arabidopsis*. Curr. Biol. *17*, 1050–1054.
9. Corbesier, L., Vincent, C., Jang, S., Fornara, F., Fan, Q., Searle, I., Giakountis, A., Farrona, S., Gissot, L., Turnbull, C., and Coupland, G. (2007). FT protein movement contributes to long-distance signaling in floral induction of *Arabidopsis*. Science *316*, 1030–1033.
10. Tamaki, S., Matsuo, S., Wong, H.L., Yokoi, S., and Shimamoto, K. (2007). Hd3a protein is a mobile flowering signal in rice. Science *316*, 1033–1036.
11. Wigge, P.A., Kim, M.C., Jaeger, K.E., Busch, W., Schmid, M., Lohmann, J.U., and Weigel, D. (2005). Integration of spatial and temporal information during floral induction in *Arabidopsis*. Science *309*, 1056–1059.
12. Abe, M., Kobayashi, Y., Yamamoto, S., Daimon, Y., Yamaguchi, A., Ikeda, Y., Ichinoki, H., Notaguchi, M., Goto, K., and Araki, T. (2005).

FD, a bZIP protein mediating signals from the floral pathway integrator FT at the shoot apex. Science *309*, 1052–1056.

13. Hilson, P., Allemeersch, J., Altmann, T., Aubourg, S., Avon, A., Beynon, J., Bhalerao, R.P., Bitton, F., Caboche, M., Cannoot, B., et al. (2004). Versatile gene-specific sequence tags for *Arabidopsis* functional genomics: transcript profiling and reverse genetics applications. Genome Res. *14*, 2176–2189.
14. Ruiz-Garcia, L., Madueno, F., Wilkinson, M., Haughn, G., Salinas, J., and Martinez-Zapater, J.M. (1997). Different roles of flowering-time genes in the activation of floral initiation genes in *Arabidopsis*. Plant Cell *9*, 1921–1934.
15. Robson, F., Costa, M.M., Hepworth, S.R., Vizir, I., Pineiro, M., Reeves, P.H., Putterill, J., and Coupland, G. (2001). Functional importance of conserved domains in the flowering-time gene CONSTANS demonstrated by analysis of mutant alleles and transgenic plants. Plant J. *28*, 619–631.
16. Kagaya, Y., Ohmiya, K., and Hattori, T. (1999). RAV1, a novel DNA-binding protein, binds to bipartite recognition sequence through two distinct DNA-binding domains uniquely found in higher plants. Nucleic Acids Res. *27*, 470–478.
17. Wenkel, S., Turck, F., Singer, K., Gissot, L., Le Gourrierec, J., Samach, A., and Coupland, G. (2006). CONSTANS and the CCAAT box binding complex share a functionally important domain and interact to regulate flowering of *Arabidopsis*. Plant Cell *18*, 2971–2984.
18. Kobayashi, Y., and Weigel, D. (2007). Move on up, it's time for change—mobile signals controlling photoperiod-dependent flowering. Genes Dev. *21*, 2371–2384.
19. Boss, P.K., Bastow, R.M., Mylne, J.S., and Dean, C. (2004). Multiple pathways in the decision to flower: enabling, promoting, and resetting. Plant Cell *16* (*Suppl*), S18–S31.
20. Ferrandiz, C., Gu, Q., Martienssen, R., and Yanofsky, M.F. (2000). Redundant regulation of meristem identity and plant architecture by FRUITFULL, APETALA1 and CAULIFLOWER. Development *127*, 725–734.